



In situ casting of polyvinyl chloride membranes in agar-bridged extended-gate field effect transistor sensors

Zahrah Jobran Alqahtani¹, Martin Grell², and Abeer Alqurashi¹

¹Physics Department, Faculty of Science, Taif University, Taif, P.O. Box 11099, 21944 Taif, Saudi Arabia

²University of Chuka, Faculty of Science & Technology, Department of Physical Sciences,
Box 109-60400, Chuka, Kenya

Correspondence: Zahrah Jobran Alqahtani (z.mousa@tu.edu.sa)

Received: 14 September 2025 – Revised: 12 January 2026 – Accepted: 12 February 2026 – Published: 31 March 2026

Abstract. The recent bridged EGFET (extended-gate field effect transistor) sensor design is the most user-friendly potentiometric transducer concept to date. Manufacturing of the sensor, the introduction of a sensitised phase transfer membrane by in situ casting, and transduction of the electric potential resulting from analyte–sensitiser binding are remarkably simple. However, so far, the immobilisation of the sensitiser has only been demonstrated within an agar hydrogel phase transfer membrane, the same material used for the so-called bridge that defines the concept. Here, we demonstrate in situ casting of a plasticised polyvinyl chloride (PVC) membrane onto the agar bridge as an alternative. We compare the performance of different types of sensitisers – an organic dye and an ion-exchanging clay – for the same target analyte, Cr(VI) oxyanions, when the sensitiser is immobilised in either an agar hydrogel or a plasticised PVC membrane. We find superior performance, as quantified by sensor response at the Cr(VI) maximum contaminant limit, when the membrane and processing solvent match the solubility of the sensitiser. We unite the simplicity of the bridged EGFET, the convenience of in situ membrane casting, and the performance advantage of organic-solvent-processed phase transfer membranes for organic sensitisers.

1 Introduction

Piet Bergveld founded the lineage of potentiometric field effect sensors with his invention of the ion-sensitive field effect transistor (ISFET) in 1970 (Bergveld, 1970). The discipline was reinvigorated by two major developments from the original concept, namely the extended-gate field effect transistor (EGFET) by Van der Spiegel et al. (1983) and the water gate thin-film transistor (WGTFT) by Kergoat et al. (2010). EGFETs and WGTFTs have since been widely applied as potentiometric sensors, including ion sensors as reviewed e.g. by Liu et al. (2022), but also for bioanalytes, as reviewed e.g. by Pullano et al. (2018). In both the EGFET and the WGTFT, the gate potential is communicated to the transistor channel capacitively across the aqueous medium under test via a pair of electric double layers (EDLs). In the EGFET, the EDL capacitor is formed externally, while in the

WGTFT, the EDL capacitor is integrated into the transistor itself, replacing the conventional gate insulator. The electric readout of both WGTFTs and EGFETs requires only simple electric equipment (source measure units, SMUs). The simplicity of DC electric readout makes the field effect highly competitive with other biosensor transducer concepts like surface plasmon resonance (SPR) (e.g. Soares et al., 2022) or electric impedance spectroscopy (e.g. Reich et al., 2017), which require rather complex instrumentation and data analysis procedures. The integration of the EDL into the WGTFT appears, at first, to be elegant, but it forces researchers to prepare the semiconducting channel themselves (e.g. Al Baroot and Grell, 2019; Alghamdi et al., 2019; Alqahtani et al., 2020a, b; Althagafi et al., 2016; Schmoltner et al., 2013). This demands significant laboratory infrastructure, and the electric performance of “do-it-yourself” transistors is limited by lower carrier mobility and longer channels. In the EGFET

approach, researchers instead employ a commercially available field effect transducer (FET) as a transducer. A recent, comprehensive review of the field effect transducers is in Grell and Alqahtani (2025).

The remaining challenge for all FET-based (and other) sensors is the introduction and immobilisation of a sensitiser (a.k.a. receptor) into the transistor architecture to impart a potentiometric response selective to a targeted waterborne analyte. For biosensors (typically proteins), this is often achieved by covalent coupling to an electrode. Covalent immobilisation is not trivial and requires expert input from biochemists, as seen in a review by, e.g., Duval et al. (2015). Alternatively, non-biological sensitisers (e.g. organic ionophores or ion exchangers) are often immobilised via entrapment in a soft synthetic polymer phase transfer matrix, e.g. silicone (Chen and Bühlmann, 2022) or plasticised polyvinyl chloride (PVC) (e.g. Alghamdi et al., 2019; Alqahtani et al., 2020a, b; Alrabiah et al., 2016; Schmoltner et al., 2013; Shahim et al., 2019; Sukesan et al., 2019), cast from organic solvent. However, the preparation and handling of free-standing soft polymer membranes for introduction into the sensor architecture are not trivial either.

The introduction of sensitisers into FET sensor architectures was recently advanced by the bridged EGFET design by Alqahtani et al. (2023) and was modified by Alqahtani et al. (2024); see Fig. 1 below. The defining bridge is formed by agar hydrogel set in a U-tube. The preparation of agar bridges is remarkably simple: agar is a widely available foodstuff and requires only water as a solvent, and agar solution is liquid at $T > 70\text{ }^{\circ}\text{C}$, which allows for the filling of a U-tube with agar solution, wherein it then sets into a soft but solid hydrogel at ambient temperature. The gel bridge allows capacitive communication between two electrically contacted water pools (sample and reference pools) in the same way as liquid water does, but it seals pools against the intermixing of their waters. A sensitiser can be immobilised by entrapment within the agar bridge (Alqahtani et al., 2023) or by in situ casting of another layer of hot agar loaded with sensitiser onto a previously set gel seal (Alqahtani et al., 2024); the details of this can be found in Sect. 2.1. This avoids the need to handle free-standing membranes as it immediately anchors and mechanically supports membranes on the spot of their use. Consequently, the bridged EGFET is the most user-friendly potentiometric transducer concept to date. However, so far, in situ casting onto an agar seal has been demonstrated only for membranes also formed of agar and not for soft polymer membranes on the agar seal, while it has been established that the type of membrane may affect performance for a given sensitiser (e.g. Alqahtani et al., 2023). Many useful sensitisers are soluble only in organic solvents and not in water, and their performance is likely to benefit from the organic processing solvent used for synthetic polymer membranes.

Therefore, here, we report the in situ casting of sensitised PVC membranes from organic solvent onto agar gel bridges as an alternative to agar-on-agar membranes, and we system-

atically compare the resulting sensor performance for different types of sensitisers entrapped in either agar or PVC membranes.

To enable meaningful comparisons between different membrane matrices, our choice of sensitisers was guided by the idea of finding two rather different types of sensitisers that respond to the same analyte. Therefore, here, we target waterborne Cr(VI) oxyanions – see Sect. 2.3 – as our analyte example. Hexavalent Cr is rare naturally but is industrially produced in large quantities for chromium processing (Anger et al., 2000) and is a highly toxic water contaminant. Consequently, Cr(VI) “maximum contaminant levels” (MCLs) of the order $50\text{ }\mu\text{g L}^{-1}$ ($\sim 1\text{ }\mu\text{M}$) are in place in many jurisdictions worldwide; an MCL for Cr(VI) of $10\text{ }\mu\text{g L}^{-1}$ ($0.19\text{ }\mu\text{M}$) is currently proposed in California (California State Water Resources Control Board, 2024). Waterborne Cr(VI) is therefore targeted by a number of sensor concepts, both potentiometric and other types; a comprehensive review is in Zhang and Li (2019).

Our choice of example analyte is justified by our identification of two different types of sensitiser for Cr(VI): Shahim et al. (2019) have already demonstrated that the organic dye Quinaldine Red (QR) acts as a sensitiser for waterborne Cr(VI). QR dissolves well in the solvent tetrahydrofuran (THF), the solvent used for plasticised PVC membranes, but not in water. On the other hand, here, we show that the natural clay “bentonite” also acts as a sensitiser for waterborne Cr(VI). As an inorganic mineral, bentonite is entirely insoluble in organic solvents but disperses well in water; see Sect. 2.2 for more detail.

Embedding two different types of sensitisers in two different membrane matrices but targeting the same analyte enables us to study the relationship between sensitiser, membrane, and processing solvent and leads to meaningful conclusions regarding the merit of in situ cast PVC membranes within the bridged EGFET concept.

2 Experimental: sensor design, material selection and in situ processing, calibration and evaluation

2.1 Potentiometric sensor design: the bridged EGFET

Here, we use the bridged EGFET (Alqahtani et al., 2023) variation of the widely used EGFET sensor design, as discussed in the Introduction, in a setup similar to that of Alqahtani et al. (2024). We use a 6.5 cm glass U-tube length with an inner diameter (ID) of 1.4 cm. We seal the U-bend with agar-agar by filling it with 7 mL of non-sensitised 20 mg mL^{-1} hot agar solution in water, allowing it to cool and set into a hydrogel. We use locally drawn tap water for agar solution; our preference for tap water over deionised (DI) water or buffers is explained in Sect. 2.3. One leg of the agar seal was then sensitised with an in situ cast membrane as described in Sect. 2.2. Both legs of the U-tube were filled with 3 mL of tap water to form two pools that are physically sep-

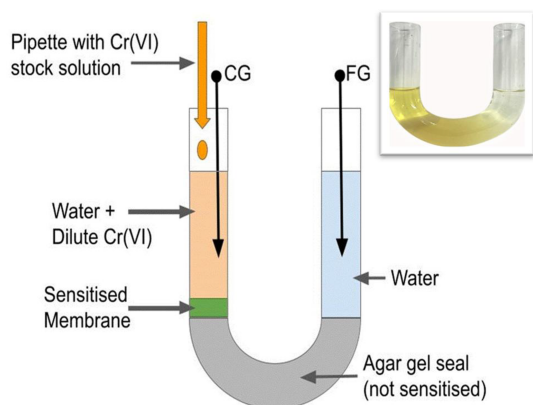


Figure 1. Schematic illustration of a bridged EGFET U-tube sensor design, similar to that of AlQahtani et al. (2024), with an agar seal in the U-bend. The U-tube design upturns the original agar bridge introduced by AlQahtani et al. (2023) into what is more akin to an underpass. However, the electric communication across the agar gel seal is independent of its orientation, and both we and AlQahtani et al. (2024) retain the term bridged EGFET. The membrane is cast in situ and is loaded with an entrapped sensitiser. Inset: photo of sensitised U-tube. The membrane is an agar hydrogel sensitised with entrapped bentonite.

arated but communicate capacitively across the agar bridge. We contact each pool with zinc (Zn) needles as electrodes. We configure the electrode on the sensitised side as a “control gate” (CG) and connect it to an Osilla P2005A2 source measure unit (SMU) to sweep V_{CG} . We configure the other electrode as a “floating gate” (FG) and connect it to the gate of an LND150 normally on n -channel MOSFET (LND150 MOSFET Datasheet pdf, 2023), a popular choice for EGFET sensors (e.g. Al-Hardan et al., 2016; AlQahtani et al., 2023, 2024; Alqahtani and Grell, 2024; Shahim et al., 2019). We ground the LND150 source and connected the drain to a second Osilla P2005A2 SMU configured as an ammeter to record the LND150 drain current I_D at constant drain voltage $V_D = 0.2$ V. We calibrate sensors by recording transfer characteristics $I_D(V_{CG})$ under increasing concentrations of Cr(VI) as analyte in the CG pool, as described in Sect. 2.3. The overall setup is illustrated in Fig. 1.

While, in previous work (AlQahtani et al., 2024), the sensitised membrane was always formed by another layer of agar hydrogel, here, we experiment with in situ cast PVC membranes as well; see Sect. 2.2. We select PVC membranes as a widely used representative of synthetic polymer membranes (e.g. Alghamdi et al., 2019; Alqahtani et al., 2020a, b; Alrabiah et al., 2016; Schmoltnner et al., 2013; Shahim et al., 2019; Sukesan et al., 2019). Alternative synthetic membranes based on silicone offer better biocompatibility (Chen and Bühlmann, 2022), but Cr(VI) oxyanions are water pollutants rather than physiological ions and so will not be quantified e.g. in human sweat, and respective applications do not demand biocompatibility.

2.2 Sensitisers for Cr(VI) and in situ membrane preparation

We identify two different sensitisers for the same analyte, aqueous Cr(VI), one an organic dye, the other an inorganic mineral; see the Introduction. This is for systematic comparison of different types of sensitisers in different membrane formulations, namely agar hydrogel vs. plasticised PVC membranes. As an organic sensitiser, we use the non-cyclic organic dye Quinaldine Red (QR), sourced from Sigma Aldrich. Shahim et al. (2019) have already shown a potentiometric EGFET sensor for Cr(VI) with QR as a sensitiser. QR dissolves well in THF, the solvent used for plasticised PVC membranes, but not in water. As an inorganic sensitiser, we use the natural mineral clay bentonite, sourced as a fine powder from Innovative Naturopathics via the Amazon store. Bentonite is known as a cation exchanger (e.g. Huertas et al., 2001; Hussain and Ali, 2021). Bentonite and derived materials are widely used sorbents for the extraction of heavy metal pollution from water; a review has been conducted by Prabhu and Prabhu (2018). While the extraction of Cr(VI) from water by bentonite and other clays is well established (Bhattacharyya and Sen Gupta, 2006), the precise mechanism is not obvious: bentonite is a cation exchanger, while Cr(VI) dissolves in water as oxyanion species; see Sect. 2.3. Memedi et al. (2017) report quantitative studies for the extraction of Cr(VI) from water by natural bentonite, consistent with the Langmuir–Freundlich sorption model; cf. Sect. 2.4. It is widely established that sorbents for a particular ion can also act as sensitisers for the same ion in WGTFTs and EGFETs (Alghamdi et al., 2019; AlQahtani et al., 2024; Alqahtani et al., 2020a, b), which will be the case here as well. We note that bentonite’s ability to sorb heavy metals from water generally rather than Cr(VI) exclusively makes it likely to give a potentiometric response to other heavy metal pollutants other than Cr(VI) as well, while QR is described as being selective for Cr(VI) by Shahim et al. (2019). However, bentonite’s lack of selectivity for Cr(VI) vs. other contaminants does not compromise the aim of our study, which is to establish the relationship between sensitiser, membrane, and processing solvent, in bridged EGFET sensors. Additionally, a “broadband” response is not always a disadvantage: a highly selective sensor for Cr(VI) would not alert the user to lead or cadmium pollution.

The solubility of bentonite contrasts with QR: bentonite is insoluble in THF. In water, bentonite does not, strictly speaking, dissolve either but disperses well. Its layered (“smectite”) structure readily allows for the diffusion of water into interlayers, where the ion exchange takes place (Nesse, 1999). We may say that water dissolves in bentonite. This also leads to interlayer expansion, i.e. swelling, resulting in viscous aqueous dispersions used, e.g., as drilling fluid.

We cast either agar or PVC membranes in situ onto the CG leg of a U-tube, with the U-bend having been previously sealed with agar hydrogel, as described in Sect. 2.1

(see Fig. 1). While this has previously been demonstrated for the agar membrane on the agar seal, in situ casting of PVC membranes onto the agar seal is a novelty introduced here. To form sensitised agar membranes, we disperse either 12 mg mL^{-1} QR or 53 mg mL^{-1} bentonite in a hot aqueous solution of 20 mg mL^{-1} agar. The aqueous agar gel was heated to 80°C prior to incorporating the QR or bentonite sensitiser. After casting, we leave the sensitised agar solution to cool down and gel at ambient temperature, forming a seamless unit with the unsensitised seal with an approximate thickness of 0.5 cm. QR disperses in agar hydrogel but does not swell or dissolve. A photo of a QR dispersion in agar is shown in Fig. S3. For a consistent experimental protocol, we left the bentonite for 2 h before use to allow swelling. Swelling is visible in the early stages, but incubation beyond 2 h did not lead to any further swelling. To form a sensitised PVC membrane, we purchased high-molecular-weight polyvinyl chloride (PVC), plasticiser 2-nitro phenyl octyl ether, and the solvent tetrahydrofuran (THF) from Sigma Aldrich. We dissolve 114 mg PVC and $144 \mu\text{L}$ plasticiser in 3 mL THF, similarly to what has been reported previously by Shahim et al. (2019), but without their anion excluder. We add 159 mg bentonite or 35 mg QR and stir for 5 min at a stirring rate of 400 rpm. Note that this is the same sensitiser weight in per mL THF as the previously used per mL water. QR weigh-in once again matches the prior work of Shahim et al. (2019). While QR dissolves in THF, giving a red solution, bentonite does not disperse well in THF. We then cast 0.5 mL of this mixture into a U-tube and store the tube for 6–8 h under ambient temperature to evaporate THF and for in situ formation of the sensitised PVC membrane. We note that, upon THF evaporation, bentonite separates into a coagulated spot in the centre of the membrane, while QR remains evenly distributed, as seen from the red colouration. The coagulation of bentonite in PVC is shown in Sect. S2 and Fig. S4 in the Supplement.

2.3 Sensor calibration

For sensor calibration, we pour locally drawn tap water into both legs of the agar bridge/sensitised membrane in the U-tube and bring it into contact with electrodes as described in Sect. 2.1. We prefer tap water to DI water as it contains a small amount of common ions that act as supporting electrolytes, enabling good capacitive communication of electric potential between the CG and FG via electric double layers. Tap water is also a rather realistic model for environmental samples. We avoid the use of buffers as they contain rather high concentrations of ions which may act as interferants and are not a realistic simulant for environmental samples. We then calibrate bridged EGFET sensors by sweeping V_{CG} from -1700 to $+400$ mV and recording LND150 transfer characteristics $I_{\text{D}}(V_{\text{CG}})$, first under pure water ($c = 0$) and then again after step-wise titration of increasing amounts of Cr(VI) stock solutions into the CG pool,

as shown in Fig. 1. We prepared three Cr(VI) stock solutions (100 mM, 1 mM, and $100 \mu\text{M}$) in locally drawn tap water from Chromium(VI)oxide, CrO_3 , sourced from Sigma Aldrich. Cr(VI) oxide and salts dissolve into water under the formation of several Cr(VI) oxyanions, namely the monovalent hydrogen chromate (HCrO_4^-) and the divalent chromate (CrO_4^{2-}) and dichromate ($\text{Cr}_2\text{O}_7^{2-}$) anions, in relative proportions that depend on concentration and pH (California State Water Resources Control Board, 2024; Zhang and Li, 2019). By concentration c of Cr(VI), we always mean total Cr(VI), regardless of how it splits into different oxyanion species. Around pH 7 and low to moderate concentrations, the divalent oxyanions dichromate and chromate dominate, and stock solutions display the yellow/orange colour typical of chromate/dichromate. While we somewhat adapted the titration range to the different sensors' response characteristics, we always included $c = \text{MCL} = 1 \mu\text{M}$ for a pragmatic assessment of sensor performance at low c ; see Sects. 2.4 and 4.

The interactions of the Cr(VI) oxyanion “cocktail” with the sensitiser immobilised at the interface between the sensitised membrane and CG leg water pool lead to a concentration-dependent interface potential $\Delta V_{\text{CG}}(c)$ that adds to the CG potential applied by the voltage source V_{CG} . The potential communicated to the FG and LND150 gate is, therefore, different from V_{CG} by $\Delta V_{\text{CG}}(c)$, shifting transfer characteristics along the V_{CG} axis. We evaluate $\Delta V_{\text{CG}}(c)$ by reading the CG voltage required to reach a particular reference drain current I_{ref} :

$$\Delta V_{\text{CG}}(c) = V_{\text{CG}}(I_{\text{D}} = I_{\text{ref}}, c) - V_{\text{CG}}(I_{\text{D}} = I_{\text{ref}}, c = 0). \quad (1)$$

$\Delta V_{\text{CG}}(c)$ evaluated in this way is independent of I_{ref} ; here, we use $I_{\text{ref}} = 0.1 \text{ mA}$ as a convenient choice. By definition, Eq. (1) is normalised to $\Delta V_{\text{CG}}(c = 0) = 0$. Normalising membrane potential shifts in this way accounts for any small differences in membrane potential due to day-to-day variations in the background ion cocktail in tap water. We read V_{CG} with an error of less than 4 mV, i.e. $\pm 2 \text{ mV}$, making error bars in our later plots of response characteristics smaller than the symbols. An empirical ΔV_{CG} of $+4 \text{ mV}$ (or more) can therefore not be ascribed to a reading error at $c = 0$. We then fit response characteristics to a theoretical model, as discussed in Sect. 2.4.

2.4 Response law fitting to sensor calibrations and sensing mechanism

The response of potentiometric sensors based on ion exchanging and other (Alqahtani et al., 2024) sensitisers results from a change in dipole moment in the sensitiser–analyte association via ion exchange. Such characteristics are commonly fitted by the Langmuir–Freundlich (LF) law (e.g. Alghamdi et al., 2019; Alqahtani et al., 2023; Alqahtani et al., 2020a, b). The LF characteristic, as shown in Eq. (2),

is a combination of the classic Freundlich (1907) and Langmuir (1918) surface adsorption isotherms to describe the fractional occupation of available sorption sites:

$$\Delta V_{CG}(c) = \Delta V_{sat} \frac{(kc)^\beta}{1 + (kc)^\beta}, \quad (2)$$

wherein ΔV_{sat} is a saturated CG shift in the limit of large analyte concentration $c \gg 1/k$, k is the sensitizer–analyte association constant, and β is a dimensionless exponent. ΔV_{CG} reaches $1/2 \Delta V_{sat}$ for $c_{1/2} = 1/k$ and saturates to ΔV_{sat} at $c \gg 1/k$. Equation (2) predicts a non-linear sensor response across the entire concentration range; hence, sensitivity also varies with concentration. LF sensors are therefore better quantified by their parameters (ΔV_{sat} , k , β) than by a linear range, which does not exist, or a sensitivity, which varies strongly with concentration.

The LF characteristic is mathematically equivalent to the Hill equation (Hill, 1910), which is the standard model in quantitative pharmacology (Gesztelyi et al., 2012) and is routinely fitted to potentiometric sensors based on biochemical interactions, such as pathogen–antibody or cancer marker–antigen binding (e.g. Zhou et al., 2019). Here, we use ORIGIN software to fit Eq. (2) to our response characteristics established as described in Sect. 2.3 and determine the LF parameters ΔV_{sat} , k , and β . We find a good fit on all occasions; parameters are reported in Figs. 2 to 5 and summarised in Table 1 below. Note, however, for $\beta < 1$, Eq. (2) formally implies a divergence in slope (i.e. sensitivity) in the limit $c \rightarrow 0$, which makes a statistical analysis of the limit of detection difficult. Instead, we report a more direct measure of sensor performance at low c ; see Sect. 4 and Table 1 below.

The response characteristics of sensors for waterborne Cr(VI) using QR as the sensitizer have previously been fitted to a Nernstian (logarithmic) response characteristic (Al-Hardan et al., 2016), with an apparently super-Nernstian response, i.e. larger than $59 \text{ mV}/z$ per decade in the analyte concentration, wherein z is the valency of the analyte ion. We believe this was based on two misunderstandings: firstly, the authors mistook waterborne Cr(VI) for “naked” Cr^{6+} cations, when, in fact Cr(VI), dissolves as monovalent or divalent oxyanions; see Sect. 2.3. Secondly, Nernstian characteristics – or their refinement, known as the Nikolsky–Eisenman (NE) law – are appropriate for ionophores that extract waterborne ions without ion exchange, thus accumulating charge. This includes pH sensors (e.g. Al-Hardan et al., 2016), as well as many metal cation sensors (e.g. Al-Baroot and Grell, 2019; Althagafi et al., 2016; Schmoltner et al., 2013) and sensors for metal oxyanions (Sukesan et al., 2019), and for organic anions (e.g. Alrabiah et al., 2016). However, QR is an organic cation with iodine as a counteranion. The association of QR with waterborne Cr(VI) oxyanions is therefore likely to be an ion exchange of iodine for chromate, with a change in dipole moment but without accumulation of charge on the sensitizer. We therefore consider the LF model to be more appropriate. A detailed discussion

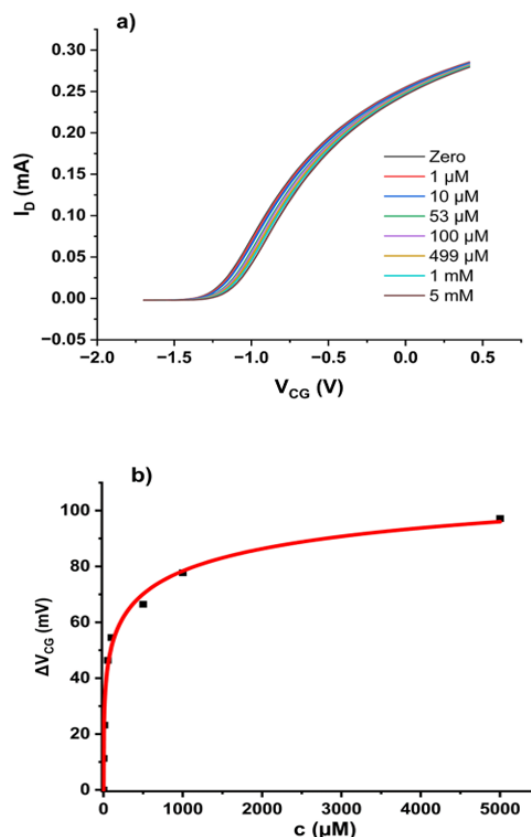


Figure 2. (a) Transfer characteristics of a bridged EGFET sensitised with QR in agar membrane under increasing Cr(VI) oxyanion concentrations. Concentration is total Cr(VI). (b) $\Delta V_{CG}(c)$ evaluated as described in Sect. 2.3. The red line shows a fit to the LF model (Eq. 2).

is in Grell and AlQahtani (2025). Consequently, we present calibration charts (later Figs. 2 to 5) on a linear concentration scale rather than on a logarithmic scale, as the former is common for LF and/or Hill characteristics, to avoid confusion with Nernstian and/or NE characteristics.

2.5 Personal protection and waste disposal

Given the toxicity and environmental harm presented by Cr(VI), our experimental work could only be carried out by following strict procedures to protect researchers from exposure and the environment from Cr(VI) waste. Cr(VI) solutions were prepared and handled exclusively in a certified chemical fume hood. Researchers wore suitable personal protective gear, including lab coats, nitrile gloves, and safety goggles. Materials and glassware that came into contact with Cr(VI) were handled with caution and collected in clearly labelled containers designated for hazardous chromium waste. Disposal of waste was carried out by an authorised hazardous waste management service, following institutional and environmental guidelines.

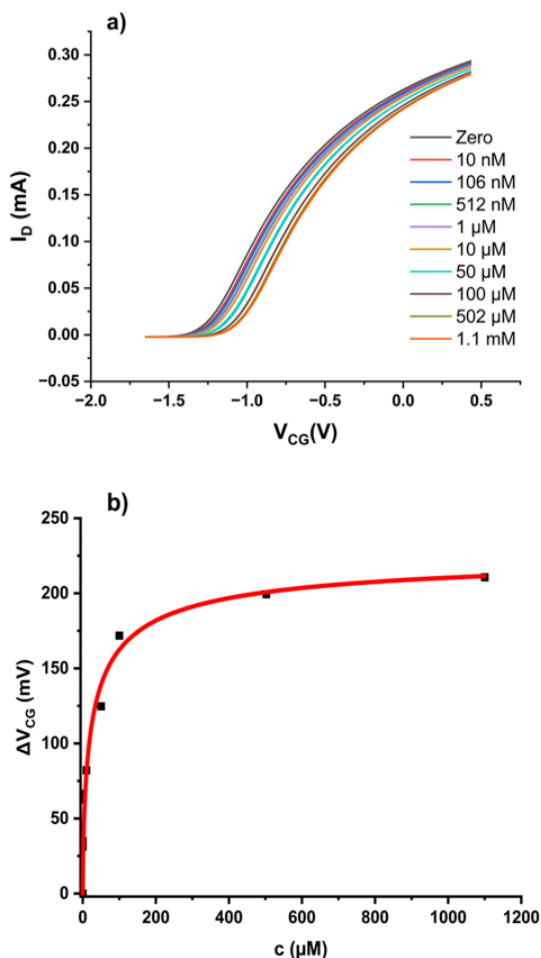


Figure 3. (a) Transfer characteristics of a bridged EGFET sensitised with QR in PVC membrane under increasing Cr(VI) oxyanion concentrations. Concentration is total Cr(VI). (b) $\Delta V_{CG}(c)$ evaluated as described in Sect. 3. The red line shows a fit to the LF model (Eq. 2).

3 Results and discussion

3.1 Bridged EGFET responses to Cr(VI) with QR in agar and PVC membranes

For a bridged EGFET such as that in Fig. 1, sensitised with QR in agar gel, as described in Sect. 2.2, we find the “family” of transfer characteristics under titration of increasing amounts of Cr(VI) into the CG pool as shown in Fig. 2a. We clearly find a response to waterborne Cr(VI). We evaluate response characteristics $\Delta V_{CG}(c)$ as described in Sect. 2.3 – see Eq. (1) – and fit against the LF model, as shown in Fig. 2b.

The LF model fits the data well. The resulting fit parameters are $\Delta V_{sat} = (136 \pm 29)$ mV, $k = (23.9 \pm 3.2) \times 10^3$ L mol⁻¹, and $\beta = 0.35 \pm 0.08$. The parameters are summarised in Table 1 below, where they are discussed in the context of other results to follow.

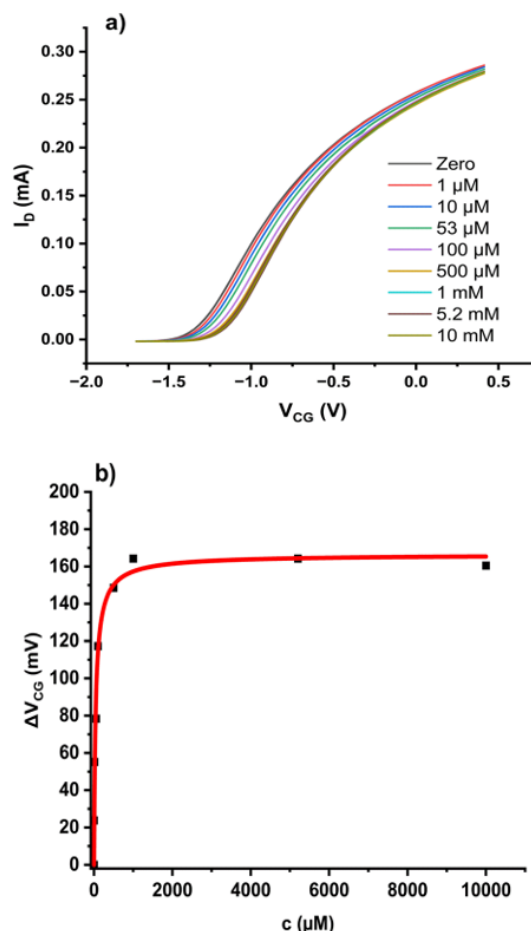


Figure 4. (a) Transfer characteristics of a bridged EGFET sensitised with bentonite in agar under an increasing concentration of Cr(VI) oxyanions. Concentration is total Cr(VI). (b) $\Delta V_{CG}(c)$ evaluated as described in Sect. 2.3. The red line is a fit to the LF model (Eq. 2).

To enable comparison between different membrane matrices, we have prepared a bridged EGFET with a PVC (instead of agar) membrane cast in situ, as described in Sect. 2.2, but again sensitised with QR. We find the “family” of transfer characteristics under titration of increasing amounts of Cr(VI) into the CG pool, as shown in Fig. 3a. We again evaluate the response characteristics $\Delta V_{CG}(c)$ as described in Sect. 2.3 and fit against the LF model, as shown in Fig. 3b.

Once again, the LF model fits the data well. The resulting fit parameters are $\Delta V_{sat} = (229.7 \pm 16.5)$ mV, $k = (38.4 \pm 9.6) \times 10^3$ L mol⁻¹, and $\beta = 0.65 \pm 0.16$. The parameters are summarised in Table 1 below, where they are discussed in context.

The good fit of LF response characteristics to QR response data in both agar and PVC membranes supports our preference for the LF over the NE model and resolves the previous claim of unexplained super-Nernstian response (Shahim et al., 2019) as the LF sensitivity has no theoretical upper limit.

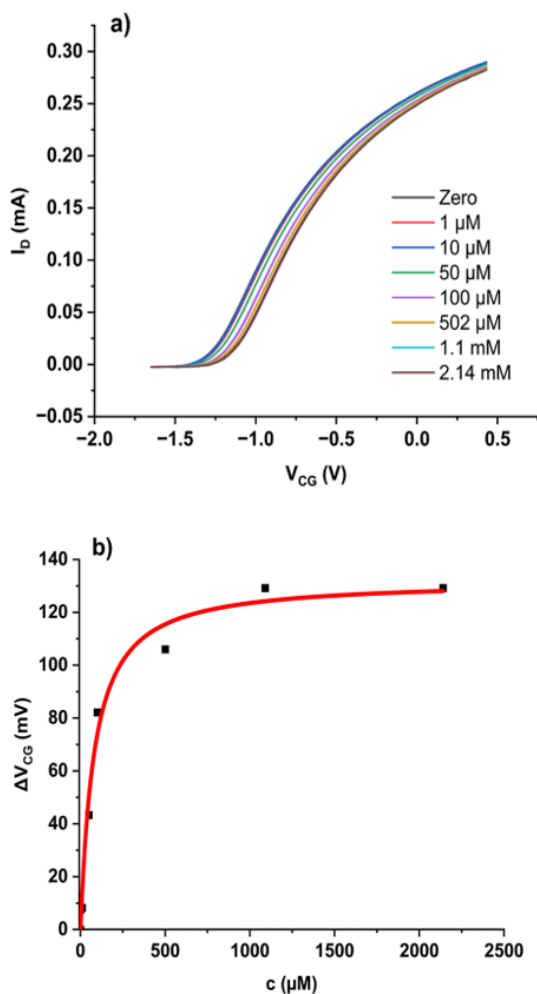


Figure 5. (a) Transfer characteristics of a bridged EGFET sensitised with bentonite in PVC under an increasing concentration of Cr(VI) oxyanions. Concentration is total Cr(VI). (b) $\Delta V_{CG}(c)$ evaluated as described in Sect. 2.3. The red line is a fit to the LF model (Eq. 2).

3.2 Bridged EGFET responses to Cr(VI) with bentonite in agar and PVC membranes

For a bridged EGFET such as that in Fig. 1, sensitised with bentonite in agar gel, as described in Sect. 2.2, we find the family of transfer characteristics under titration of increasing amounts of Cr(VI) into the CG pool, as shown in Fig. 4a. We evaluate response characteristics $\Delta V_{CG}(c)$ as described in Sect. 2.3 – see Eq. (1) – and fit against the LF model, as shown in Fig. 4b.

The resulting fit parameters are $\Delta V_{sat} = (166.6 \pm 5.5)$ mV, $k = (23.2 \pm 4) \times 10^3$ L mol⁻¹, and $\beta = 0.89 \pm 0.18$. The parameters are summarised in Table 1 below, where they are discussed in context.

As an alternative, we have prepared a bentonite-sensitised bridged EGFET with a PVC membrane cast in situ as described in Sect. 2.2. We find the family of transfer character-

istics under titration of increasing amounts of Cr(VI) into the CG pool, as shown in Fig. 5a. We again evaluate the response characteristics $\Delta V_{CG}(c)$ as described in Sect. 2.3 and fit them against the LF model, as shown in Fig. 5b.

The resulting fit parameters are $\Delta V_{sat} = (132 \pm 8.5)$ mV, $k = (12.5 \pm 2.8) \times 10^3$ L mol⁻¹, and $\beta = 1.05 \pm 0.27$. The parameters are summarised in Table 1, where they are discussed in context.

3.3 Repeatability, response time, and stability

When we prepare nominally identical devices twice, the response characteristics are very similar to each other. All sensors reported here respond to the addition of analyte with a shift in their transfers on a timescale shorter than the recording of a transfer characteristic. When no further analyte is added, the transfer shift remains constant for a timescale longer than needed for a full calibration. We demonstrated repeatability, fast response, and stability in the Supplement (Sect. S1).

4 Comparison between membrane matrices and discussion

For comparison and discussion, we summarise all LF fit parameters evaluated from Figs. 2 to 5, including confidence intervals, in Table 1.

Generally, better performance of a sensor is indicated by higher ΔV_{sat} and larger k (i.e. smaller $c_{1/2} = 1/k$). As a practical comparator, Table 1 also includes $\Delta V_{CG}(1 \mu\text{M})$, i.e. the sensor response at $c = 1 \mu\text{M} = \text{MCL}$. $\Delta V_{CG}(1 \mu\text{M})$ is read directly from Figs. 2a to 5a. We prefer a direct empirical measure of sensor performance at low c over a statistical evaluation of a limit of detection as this is difficult for an LF law; see Sect. 2.4.

The configuration with the best performance is the QR sensitiser in PVC membrane. However, in all cases, the response at MCL is larger than our reading error of 4 mV (see Sect. 2.3), which means all sensors are capable, in principle, of deciding the “potability” of water with respect to Cr(VI).

The entries in Table 1 enable a comparison of sensor performance between different membranes and sensitisers. Comparing sensors sensitised with QR in different membranes, we clearly find a response for QR in agar despite the lack of solubility of QR in water. The sensing mechanism, presumably ion exchange (see Sect. 2.4), appears to be effective even when it can occur only at the interface between dispersed QR grains and the hydrogel matrix. However, the sensor with the QR in PVC outperforms the QR-in-agar sensor across all performance metrics. The practically relevant response at the MCL is ~ 6 times larger in plasticised PVC than in the agar membrane. Sensor performance benefits from processing the organic sensitiser in an organic solvent, where it truly dissolves, rather than in water, where QR only disperses rather than dissolves during processing.

Table 1. LF fitting parameters and confidence intervals derived from Figs. 2–5.

Figure	Sensitiser	Membrane	ΔV_{sat} [mV]	k [10^3 L mol^{-1}]	β	$\Delta V_{\text{CG}} (1 \mu\text{M})$ [mV]
2	QR	Agar	136 ± 29	23.9 ± 3.2	0.35 ± 0.08	11.3
3	QR	PVC	230 ± 17	38.4 ± 9.6	0.65 ± 0.16	67
4	Bentonite	Agar	167 ± 6	23.2 ± 4	0.89 ± 0.18	18.8
5	Bentonite	PVC	132 ± 9	12.5 ± 2.8	1.05 ± 0.27	7.5

For bentonite as a sensitiser, we find somewhat better performance in an agar hydrogel membrane than in plasticised PVC. While bentonite does not strictly dissolve in water, it disperses much better in the aqueous processing medium of agar hydrogel than in the organic solvent THF used to cast plasticised PVC membranes; see Sect. 2.2.

In either case, we find better performance when we choose a membrane matrix with a processing solvent matched to the solubility of the sensitiser.

5 Summary and conclusions

Our experimental design – two sensitisers for the same analyte but with different solubility – is motivated by our aim to explore the relation between sensitiser solubility in the membrane processing solvent and the resulting sensor performance. We find that, unsurprisingly, sensors benefit from an adequate choice of the phase transfer membrane matrix: we shall choose a membrane matrix that is processed from a solvent wherein the sensitiser dissolves or, at least, disperses well. However, in the agar-bridged EGFET design, so far, only hydrogel membranes, which are processed from water, have been implemented. Water or aqueous media, such as phosphate-buffered saline (PBS), constitute adequate solvents or media for the dispersion of proteins, mineral sensitisers, or metal-organic frameworks but not for organic sensitisers like QR, which are insoluble in water.

Here, we overcome this limitation by means of the in situ casting of a PVC phase transfer matrix from organic solvent (here, THF) onto an agar hydrogel bridge. For the example of the QR sensitiser for Cr(VI), we combine the simplicity of the bridged EGFET and the convenience of in situ membrane casting with the performance advantage of processing QR from an organic solvent. While this is demonstrated here based on the specific example of QR for Cr(VI), we are confident that the in situ casting of PVC (or other synthetic polymer) membranes can be generalised to other sensitisers that are soluble in organic solvents but insoluble in water. This extends the future scope of agar-bridged EGFET sensors beyond water-processed sensitisers. For sensitisers that dissolve, swell, or disperse well in water but are insoluble in organic solvents, we instead recommend immobilising the sensitiser in agar hydrogel, like in previous reports (Alqahtani et al., 2023, 2024).

Code availability. No specific software code was developed for this research.

Data availability. All the data in this work were generated by the authors and are available in Figs. 2–5 and Table 1 in the present paper, and in Figs. S1 to S4.

Supplement. The supplement related to this article is available online at <https://doi.org/10.5194/jsss-15-67-2026-supplement>.

Author contributions. Conceptualisation: ZA and MG. Methodology: ZA, MG, and AA. Formal analysis: ZA and MG. Investigation: ZA and MG. Resources: ZA. Data curation: MG. Writing (original draft preparation): MG. Writing (review and editing): MG and ZA. Supervision: MG. Project administration: ZA. Funding acquisition: ZA.

Competing interests. The contact author has declared that none of the authors has any competing interests.

Disclaimer. Publisher's note: Copernicus Publications remains neutral with regard to jurisdictional claims made in the text, published maps, institutional affiliations, or any other geographical representation in this paper. The authors bear the ultimate responsibility for providing appropriate place names. Views expressed in the text are those of the authors and do not necessarily reflect the views of the publisher.

Acknowledgements. The authors would like to acknowledge the Deanship of Graduate Studies and Scientific Research, Taif University, for funding this work.

Financial support. Zahrah Alqahtani's research has been supported financially by the Deanship of Graduate Studies and Scientific Research, Taif University.

Review statement. This paper was edited by Michele Penza and reviewed by three anonymous referees.

References

- Al Baroot, A. F. and Grell, M.: Comparing electron- and hole transporting semiconductors in ion sensitive water-gated transistors, *Mater. Sci. Semiconduct. Process.*, 89, 216–222, <https://doi.org/10.1016/j.mssp.2018.09.018>, 2019.
- Alghamdi, N., Alqahtani, Z., and Grell, M.: Sub-nanomolar detection of cesium with water-gated transistor, *J. Appl. Phys.*, 126, 064502, <https://doi.org/10.1063/1.5108730>, 2019.
- Al-Hardan, N., Abdul Hamid, M., Ahmed, N., Jalar, A., Shamsudin, R., Othman, N., Kar Keng, L., Chiu, W., and Al-Rawi, H.: High Sensitivity pH Sensor Based on Porous Silicon (PSi) Extended Gate Field-Effect Transistor, *Sensors*, 16, 839, <https://doi.org/10.3390/s16060839>, 2016.
- AlQahtani, H. R., Al-Odayni, A.-B. M., Alhamed, Y., and Grell, M.: Bridged EGFET Design for the Rapid Screening of Sorbents as Sensitisers in Water-Pollution Sensors, *Sensors*, 23, 7554, <https://doi.org/10.3390/s23177554>, 2023.
- AlQahtani, H. R., Al-Odayni, A.-B. M., Zeama, M., Shekhah, O., Eddaoudi, M., and Grell, M.: Metal-organic frameworks as sensitizers for potentiometric sensors, *Microchem. J.*, 201, 110547, <https://doi.org/10.1016/j.microc.2024.110547>, 2024.
- Alqahtani, Z. and Grell, M.: A ‘Frugal’ EGFET Sensor for Waterborne H₂S, *Sensors*, 24, 407, <https://doi.org/10.3390/s24020407>, 2024.
- Alqahtani, Z., Alghamdi, N., and Grell, M.: Monitoring the lead-and-copper rule with a water-gated field effect transistor, *J. Water Health*, 18, 159–171, <https://doi.org/10.2166/wh.2020.186>, 2020a.
- Alqahtani, Z., Alghamdi, N., Robshaw, T. J., Dawson, R., Ogden, M. D., Buckley, A., and Grell, M.: Water-Gated Transistor Using Ion Exchange Resin for Potentiometric Fluoride Sensing, *Micro-machines*, 11, 923, <https://doi.org/10.3390/mi11100923>, 2020b.
- Alrabiah, H., Al-Majed, A., Abounassif, M., and Mostafa, G. A. E.: Ionophore-based potentiometric PVC membrane sensors for determination of phenobarbitone in pharmaceutical formulations, *Acta Pharmaceut.*, 66, 503–514, <https://doi.org/10.1515/acph-2016-0042>, 2016.
- Althagafi, T. M., Al Baroot, A. F., Algarni, S. A., and Grell, M.: A membrane-free cation selective water-gated transistor, *Analyst*, 141, 5571–5576, <https://doi.org/10.1039/C6AN00967K>, 2016.
- Anger, G., Halstenberg, J., Hochgeschwender, K., Scherhag, C., Korallus, U., Knopf, H., Schmidt, P., and Ohlinger, M.: Chromium Compounds, in: *Ullmann’s Encyclopedia of Industrial Chemistry*, Wiley-VCH Verlag GmbH & Co., ISBN 978-3-527-32943-4, https://doi.org/10.1002/14356007.a07_067, 2000.
- Bergveld, P.: Development of an Ion-Sensitive Solid-State Device for Neurophysiological Measurements, *IEEE T. Biomed. Eng.*, BME-17, 70–71, <https://doi.org/10.1109/TBME.1970.4502688>, 1970.
- Bhattacharyya, K. G. and Sen Gupta, S.: Adsorption of Chromium(VI) from Water by Clays, *Ind. Eng. Chem. Res.*, 45, 7232–7240, <https://doi.org/10.1021/ie060586j>, 2006.
- California State Water Resources Control Board: Hexavalent Chromium (Chromium-6), https://www.waterboards.ca.gov/drinking_water/certlic/drinkingwater/Chromium6.html (last access: 14 August 2024), 2024.
- Chen, X. V. and Bühlmann, P.: Ion-selective potentiometric sensors with silicone sensing membranes: A review, *Curr. Opin. Electrochem.*, 32, 100896, <https://doi.org/10.1016/j.coelec.2021.100896>, 2022.
- Duval, F., Van Beek, T. A., and Zuilhof, H.: Key steps towards the oriented immobilization of antibodies using boronic acids, *Analyst*, 140, 6467–6472, <https://doi.org/10.1039/C5AN00589B>, 2015.
- Freundlich, H.: Über die Adsorption in Lösungen, *Z. Phys. Chem.*, 57U, 385–470, <https://doi.org/10.1515/zpch-1907-5723>, 1907.
- Geszteyi, R., Zsuga, J., Kemeny-Beke, A., Varga, B., Juhasz, B., and Tosaki, A.: The Hill equation and the origin of quantitative pharmacology, *Arch. Hist. Exact Sci.*, 66, 427–438, <https://doi.org/10.1007/s00407-012-0098-5>, 2012.
- Grell, M. and AlQahtani, H. R.: The field effect transducer “family” in the aqueous medium, in: *Electrochemical Sensors and Biosensors*, Elsevier, 271–320, <https://doi.org/10.1016/B978-0-443-31562-6.00011-3>, 2025.
- Hill, A. V.: A new mathematical treatment of changes of ionic concentration in muscle and nerve under the action of electric currents, with a theory as to their mode of excitation, *J. Physiol.*, 40, 190–224, <https://doi.org/10.1113/jphysiol.1910.sp001366>, 1910.
- Huertas, F. J., Carretero, P., Delgado, J., Linares, J., and Samper, J.: An Experimental Study on the Ion-Exchange Behavior of the Smectite of Cabo de Gata (Almería, Spain): FEBEX Bentonite, *J. Colloid Interf. Sci.*, 239, 409–416, <https://doi.org/10.1006/jcis.2001.7605>, 2001.
- Hussain, S. and Ali, S.: Removal of Heavy Metal by Ion Exchange Using Bentonite Clay, *J. Ecol. Eng.*, 22, 104–111, <https://doi.org/10.12911/22998993/128865>, 2021.
- Kergoat, L., Herlogsson, L., Braga, D., Piro, B., Pham, M.-C., Crispin, X., Berggren, M., and Horowitz, G.: A Water-Gate Organic Field-Effect Transistor, *Adv. Mater.*, 22, 2565–2569, <https://doi.org/10.1002/adma.200904163>, 2010.
- Langmuir, I.: The adsorption of gases on plane surfaces of glass, mica and platinum, *J. Am. Chem. Soc.*, 40, 1361–1403, <https://doi.org/10.1021/ja02242a004>, 1918.
- Liu, C., Ye, Z., Wei, X., and Mao, S.: Recent advances in field-effect transistor sensing strategies for fast and highly efficient analysis of heavy metal ions, *Electrochem. Sci. Adv.*, 2, e2100137, <https://doi.org/10.1002/elsa.202100137>, 2022.
- LND150 MOSFET Datasheet pdf: Depletion-Mode MOSFET. Equivalent, Catalog, <https://datasheetspdf.com/pdf/60292/SupertexInc/LND150/1> (last access: 6 October 2023), 2023.
- Memedi, H., Atkovska, K., Lisichkov, K., Marinkovski, M., Kuvendziev, S., Bozinovski, Z., and Reka, A. A.: Separation of Cr(VI) From Aqueous Solutions by Natural Bentonite: Equilibrium Study, *Qual. Life*, 8, 41–47, <https://doi.org/10.7251/QOL1701041M>, 2017.
- Nesse, W. D.: *Introduction to Mineralogy*, Oxford University Press, New York, ISBN 20 978-0-19-510691-6, 1999.
- Prabhu, P. P. and Prabhu, B.: A Review on Removal of Heavy Metal Ions from Waste Water using Natural/Modified Bentonite, *MATEC Web Conf.*, 144, 02021, <https://doi.org/10.1051/mateconf/201814402021>, 2018.
- Pullano, S. A., Critello, C. D., Mahbub, I., Tasneem, N. T., Shamsir, S., Islam, S. K., Greco, M., and Fiorillo, A. S.: EGFET-Based Sensors for Bioanalytical Applications: A Review, *Sensors*, 18, 4042, <https://doi.org/10.3390/s18114042>, 2018.
- Reich, P., Stoltenburg, R., Strehlitz, B., Frense, D., and Beckmann, D.: Development of An Impedimetric Aptasensor for the De-

- tection of *Staphylococcus aureus*, *Int. J. Molec. Sci.*, 18, 2484, <https://doi.org/10.3390/ijms18112484>, 2017.
- Schmoltner, K., Kofler, J., Klug, A., and List-Kratochvil, E. J. W.: Electrolyte-Gated Organic Field-Effect Transistor for Selective Reversible Ion Detection, *Adv. Mater.*, 25, 6895–6899, <https://doi.org/10.1002/adma.201303281>, 2013.
- Shahim, S., Sukesan, R., Sarangadharan, I., and Wang, Y.-L.: Multiplexed Ultra-Sensitive Detection of Cr(III) and Cr(VI) Ion by FET Sensor Array in a Liquid Medium, *Sensors*, 19, 1969, <https://doi.org/10.3390/s19091969>, 2019.
- Soares, M. S., Silva, L. C. B., Vidal, M., Loyez, M., Facão, M., Caucheteur, C., Segatto, M. E. V., Costa, F. M., Leitão, C., Pereira, S. O., Santos, N. F., and Marques, C. A. F.: Label-free plasmonic immunosensor for cortisol detection in a D-shaped optical fiber, *Biomed. Opt. Exp.*, 13, 3259–3274, <https://doi.org/10.1364/BOE.456253>, 2022.
- Sukesan, R., Chen, Y.-T., Shahim, S., Wang, S.-L., Sarangadharan, I., and Wang, Y.-L.: Instant Mercury Ion Detection in Industrial Waste Water with a Microchip Using Extended Gate Field-Effect Transistors and a Portable Device, *Sensors*, 19, 2209, <https://doi.org/10.3390/s19092209>, 2019.
- Van der Spiegel, J., Lauks, I., Chan, P., and Babic, D.: The extended gate chemically sensitive field effect transistor as multi-species microprobe, *Sensors Actuat.*, 4, 291–298, [https://doi.org/10.1016/0250-6874\(83\)85035-5](https://doi.org/10.1016/0250-6874(83)85035-5), 1983.
- Zhang, J. and Li, S.: Sensors for detection of Cr(VI) in water: a review, *Int. J. Environ. Anal. Chem.*, 101, 1051–1073, <https://doi.org/10.1080/03067319.2019.1675652>, 2019.
- Zhou, L., Wang, K., Sun, H., Zhao, S., Chen, X., Qian, D., Mao, H., and Zhao, J.: Novel Graphene Biosensor Based on the Functionalization of Multifunctional Nano-bovine Serum Albumin for the Highly Sensitive Detection of Cancer Biomarkers, *Nano-Micro Lett.*, 11, 20, <https://doi.org/10.1007/s40820-019-0250-8>, 2019.